The Journal of Experimental Biology 210, 3805-3820
Published by The Company of Biologists 2007
doi:10.1242/jeb.005439

Assessment of sperm chemokinesis with exposure to jelly coats of sea urchin eggs and resact: a microfluidic experiment and numerical study

Munish V. Inamdar[1], Taeyong Kim[1], Yao-Kuang Chung[2], Alex M. Was[1], Xinran Xiang[2], Chia-Wei Wang[1], Shuichi Takayama[2], Christian M. Lastoskie[2,3], Florence I. M. Thomas[5] and Ann Marie Sastry[1,2,4,*]

[1]Department of Mechanical Engineering, [2]Department of Biomedical Engineering, [3]Department of Civil and Environmental Engineering and [4]Department of Materials Science and Engineering, University of Michigan, Ann Arbor, 48109 MI, USA and [5]Hawaii Institute of Marine Biology, University of Hawaii at Manoa, HI, USA

*Author for correspondence (e-mail: amsastry@umich.edu)

Accepted 19 July 2007

Summary

Specific peptides contained within the extracellular layer, or jelly coat, of a sea urchin egg have been hypothesized to play an important role in fertilization, though separate accounting of the effects of chemoattraction, chemokinesis, sperm agglomeration and the other possible roles of the jelly coat have not been reported. In the present study, we used a microfluidic device that allowed determination of the differences in the diffusion coefficients of sperm of the purple sea urchin *Arbacia punctulata* subjected to two chemoattractants, namely the jelly coat and resact. Our objectives were twofold: (1) to experimentally determine and compare the diffusion coefficients of *Arbacia punctulata* spermatozoa in seawater, jelly coat solution and resact solution; and (2) to determine the effect of sea urchin sperm diffusion coefficient and egg size on the sperm–egg collision frequency using stochastic simulations. Numerical values of the diffusion coefficients obtained by diffusing the spermatozoa in seawater, resact solution and jelly coat solution were used to quantify the chemotactic effect. This allowed direct incorporation of known enlargements of the egg, and altered sperm diffusion coefficients in the presence of chemoattractant, in the stochastic simulations. Simulation results showed that increase in diffusion coefficient values and egg diameter values increased the collision frequency. From the simulation results, we concluded that type of sperm, egg diameter and diffusion coefficient are significant factors in egg fertilization. Increasing the motility of sperm appears to be the prominent role of the jelly coat.

Key words: *Arbacia punctulata*, chemokinesis, microfluidics, sperm, stochastic simulations.

Introduction

Specific peptides contained within the extracellular layer, or jelly coat, of a sea urchin egg have been hypothesized to play an important role in fertilization, though separate accounting of the effects of chemoattraction, chemokinesis, sperm agglomeration and the other possible roles of the jelly coat have not been reported. In the purple sea urchin *Arbacia punctulata*, a specific peptide, resact, has been shown to increase the rate of respiration (Shimomura et al., 1986; Shimomura and Garbers, 1986; Suzuki and Garbers, 1984; Suzuki et al., 1984; Ward et al., 1985), to introduce a reorientation in a travel direction towards the resact gradient (Cook et al., 1994; Vacquier, 1998), and to increase the number of spermatozoa near the highest resact concentration (Ward et al., 1985). All of these studies have focused on resact as the putative chemoattractant within the jelly coat.

Other possible roles of the jelly coat include protection from mechanical stresses (Thomas and Bolton, 1999; Thomas et al., 1999), prevention of polyspermy (Schuel, 1984), and increasing the effective diameter of the egg for higher sperm–egg collision frequency (Farley and Levitan, 2001; Podolsky, 2001; Podolsky, 2002). It is yet to be established whether one of these roles is more important or whether under certain circumstances a particular role is more dominant than the others. Our group has investigated the role of the jelly coat in providing mechanical protection to the egg (Thomas and Bolton, 1999; Thomas et al., 1999; Thomas et al., 2001). Other researchers have investigated the target enlargement role of the jelly coat.

The presence of the jelly coat results in target (egg) enlargement; this effect has been investigated using standard egg fertilization assays (Vogel et al., 1982; Farley and Levitan, 2001; Podolsky, 2001). This technique involves treating sea urchin eggs, with and without jelly coats, with sperm solutions and then quantifying the number of fertilized eggs as a measure of sperm–egg collisions. Three main models (Farley, 2002; Hultin, 1956; Rothschild and Swann, 1951; Vogel et al., 1982) have been developed to determine the fraction of eggs fertilized based upon the sperm–egg collision frequency. Of these, the

VCCW model (Vogel et al., 1982) has been widely used and expanded upon by other workers (Farley, 2002). This model is an application of chemical kinetics to the sperm–egg reaction. A newer semi-empirical model, with assumed effects of factors affecting the fertilizability, was proposed to account for the role of jelly coats on the sperm–egg collision frequency (Podolsky, 2004).

Prior work: experiments and analytical studies

Motion of sperm toward eggs, and white blood cells toward infections (Kirkman-Brown et al., 2003), are all examples of known chemotactic phenomena, but perhaps the most detailed experimental and modeling studies have been conducted on chemotactic motion of bacteria toward nutrients (Lewus and Ford, 2001). Experimental methods fall in two broad categories, including (1) the use of capillary tubes and stopped flow devices (Adler, 1969; Adler, 1973; Ford et al., 1991; Lewus and Ford, 2001) to estimate the motility coefficient; and (2) the use of diffusion gradient devices (chamber) to determine the motility coefficient of bacteria (Ford and Lauffenburger, 1991; Lewus and Ford, 2001; Schmidt et al., 1997; Widman et al., 1997; Roush et al., 2006). Analytical and numerical models include the use of bacterial tumbling frequency (Chen et al., 1999; Chen et al., 2003; Hillen, 1996), random walk studies (Hill and Häder, 1997; Rivero et al., 1989) and coupled partial differential equations (PDEs) (Chalub et al., 2004; Ford and Lauffenburger, 1991; Schnitzer, 1993). A representative list of earlier studies dealing with the determination of the diffusion coefficients of bacteria is shown in Table 1. Apart from these studies, the molecular basis of motility and chemotaxis has been studied extensively for organisms such as *Escherichia coli* (MacNab, 1996; Parkinson, 1993; Stock and Surette, 1996).

In contrast to models and experiments in which large numbers of bacteria are considered to characterize effective diffusion, experimental studies of resact-induced chemotaxis of sperm have been conducted mainly on a single spermatozoon. For example, monitoring the biochemical response of a sea urchin spermatozoon in the form of changes in respiration rate, Ca^{2+} influx and cyclic GMP activities (Kaupp et al., 2003), estimation of the change in velocity and circling diameters of a spermatozoon (Cook et al., 1994; Kaupp et al., 2003) have all been conducted by consideration of behaviors of a single spermatozoon. We found no prior reports of aggregate behavior of *Arbacia punctulata* sperm, needed to address the questions of the effect of individual sperm motility on rates of collision, and thus, fertilization.

Apart from chemotaxis, another mechanism by which the chemoattractant affects the bacterial motion is chemokinesis. Unlike chemotaxis, the bacterial cells, when undergoing chemokinesis, do not exhibit preferential motion along the chemoattractant gradient but they show increase in the speed. The tumbling frequency remains unaffected by the presence of the chemoattractant gradient and hence the bacterial motion under chemokinesis at the individual cell level can be studied using random walk. Such chemoattractants are sometimes called chemokinetic compounds (Brown et al., 1993). Similar to chemotaxis, extensive experimental chemokinesis studies of bacterial and cellular motion exist in the literature, some of which include its application to human sperm (Ralt et al., 1994), human neural cells (Richards et al., 2004), leucocytes (Wilkinson, 1990) and *Rhodobacter sphaeroides* (Brown et al., 1993). Recently, a comparative simulation study of chemotaxis and chemokinesis in bacteria was reported (D'Orsogna et al., 2003).

In the present study, we used a microfluidic device that allowed determination of the differences in the diffusion coefficients of sperm of the purple sea urchin *Arbacia punctulata* subjected to two chemoattractants, namely the jelly coat and resact. The media (i.e. artificial seawater, jelly coat or resact solution) in the microfluidic devise were the same as the one used to prepare the sperm samples. Thus, this work comprises a study of chemokinesis. The sperm motion was quantified by analyzing the diffusive motion of sperm in the microfluidic device. The basic principle of diffusion at a particle level is mathematically analogous to bacterial/cellular motion (Schmidt et al., 1997), although the mechanisms are different. Diffusion is the outcome of the particle motion due to thermal energy, whereas cells are self-propelled (Lauffenburger et al., 1981). To distinguish between molecular diffusion and cellular random motility, the diffusion coefficient in the diffusion equation is replaced by the random motility coefficient (or simply, motility coefficient). In prior studies of bacteria and cells, it has been customary to quantify motility using the random motility coefficient; in the present work, we followed

Table 1. *A representative list of previous studies dealing with the experimental and the theoretical studies of random diffusion of bacteria*

Study	Animal/species	Method
(Roush et al., 2006)	*Pseudomonas stutzeri* KC	Chemotaxis study using a diffusion gradient chamber and solution to the governing partial differential equation
(Lewis and Ford, 2001)	Wild-type and AW405 *E. coli*	Chemotaxis analysis using a stopped flow diffusion chamber, study of motion of bacteria and capillary assay to access the bacterial response to chemoattractants
(Hill and Häder, 1997)	*Chlamydomonas nivalis* and *Peridinium gatunense*	Experimental study of a single cell motion
(Schmidt et al., 1997)	*Pseudomonas stutzeri* KC and HCB 137 *E. coli*	Bacterial diffusion with the help of two capillary tubes
(Widman et al., 1997)	HCB 33 *E. coli*	Bacterial diffusion in a diffusion gradient chamber (DGC)
(Rivero et al., 1989)	Flagellar bacteria and polymorphonuclear leukocytes	One dimensional probabilistic model of motion of flagellar species
(Adler, 1969)	Wild-type and W3110 *E. coli*	Bacterial diffusion in a capillary tube containing chemoattractant

more recent work specifically on sperm cells (Riedel et al., 2005) and used the term, diffusion coefficient, to quantify the motion of *Arbacia punctulata* sperm. We further note that random motility and diffusion coefficient have the identical dimensions of length^2/time. We also note that sea urchin sperm motion does involve running and tumbling motions; hence, the diffusion coefficient determined for sea urchin sperm is actually the effective diffusion coefficient (or effective diffusivity).

Objectives of the present study

To the best of the authors' knowledge, no study has been reported that considers both the effects of stochastic motion of the spermatozoa and egg enlargement on collision frequency. Thus, our work has the following objectives: (1) to experimentally determine and compare the diffusion coefficients of *Arbacia punctulata* spermatozoa in seawater, jelly coat solution and resact solution; and (2) to determine the effect of sea urchin sperm diffusion coefficient and egg size on the sperm–egg collision frequency using stochastic simulations. Numerical values of the diffusion coefficients obtained by diffusing the spermatozoa in seawater, resact solution and jelly coat solution, were used to quantify the chemotactic effect. This allowed direct incorporation of both known enlargements of the egg and altered sperm diffusion coefficients in the presence of chemoattractant.

Materials and methods

Specimen maintenance and gamete collection

Arbacia punctulata Lamarck 1816 were purchased from Gulf Specimen Marine Laboratory, Panacea, Florida, USA. Sea urchins were kept in the artificial seawater (ASW) tanks (salinity 33–36 p.p.t. and temperature 18–20.5°C) and fed with dry weed. To obtain sperm and eggs, individual sea urchins were selected randomly and 0.1 ml of 0.5 mol l^{-1} KCl was injected in the coelomic cavity (U-100 insulin syringe 28G1/2, Becton Dickinson and Company, Franklin Lakes, NJ, USA). If the initial injection failed to induce spawning, another 0.05 ml KCl was injected, twice, at most. If a sea urchin did not respond to 0.2 ml, the animal was returned to the tank. Eggs or sperm were collected from the spawned animals in air using a pipette. Collected eggs and sperm (referred to as dry eggs and dry sperm) were stored at 4°C in a vial in the collected conditions. The collected gametes were used to prepare the media for diffusion experiments.

The jelly coat solution was obtained from the collected eggs. First the jelly coats around collected eggs were dissolved in 500 μl artificial seawater (ASW). This parent jelly coat solution was used to obtain 750×, 500× and 250× diluted jelly coat solutions for diffusion experiments. Resact solutions of 25 nmol l^{-1} and 250 nmol l^{-1} concentration were prepared using solid resact, purchased from Phoenix Pharmaceuticals Inc., Balmont, CA, USA. Sperm samples for diffusion experiments were prepared in ASW, resact and jelly coat solutions by mixing 10 μl dry sperm with 100 μl of respective medium. See Appendix A for the detailed method of media preparation.

Diffusion coefficient experiments

The diffusion experiments were performed using a microfluidic device. This device was a modified version of the device developed as human sperm sorters. Appendix B describes the detailed method of apparatus fabrication. This device is shown schematically in Fig. 1. Preparation of the microfluidic device required the surface preparation. The device channel and reservoirs were filled and incubated with 5% bovine serum albumin (BSA, fraction V, Sigma) in phosphate-buffered saline (PBS; Invitrogen, Carlsbad, CA, USA) for at least 30 min to make the surfaces hydrophilic to reduce bubble formation and to passivate the surfaces against non-specific adsorption of sperm. After 30 min of incubation, excess BSA was rinsed away using distilled water to clear the migration channel; compressed air was blown in the channel to remove any distilled water droplets. This process was repeated, with ASW as a rinse.

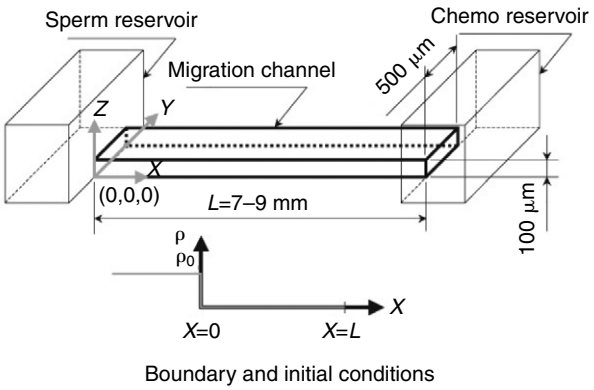

Fig. 1. The PDMS diffusion device, with dimensions, showing the chemochamber (reservoir), the migration channel and the sperm chamber (reservoir). Boundary and initial conditions used to solve the 1D diffusion equation (see Materials and methods) are also shown.

The diffusion experiments were carried out as follows. The two chambers and the migration channel were filled with ASW, whereupon the top of the chemochamber was sealed using cellophane tape (Scotch® permanent double-sided tape) and the microfluidic device was placed on the inverted microscope (TS 100, Nikon, Melville, NY, USA). The migration channel was observed for a possible flow of ASW. After confirming that the flow was not present, the sperm chamber was emptied using a pipette, and the device was observed again. This was done to ensure that the chemochamber top was properly sealed, preventing the flow in the migration channel.

Confirmation of sperm viability and tracking of sperm motion was accomplished after filling the sperm chamber with sperm solution using a syringe, and using digital image analysis. After the sperm injection, a few highly motile and individual spermatozoa appeared in the migration channel. After ~2 min, a coherent mass of spermatozoa appeared in the migration channel, which we denote hereafter as 'bulk sperm' (shown schematically in Fig. 2). This behavior of the sea urchin spermatozoa was characterized using two diffusion coefficients. The diffusion coefficient D_{motile} was determined for the first group of sperm, which we refer to as 'highly motile sperm.' The diffusion coefficient D was determined for bulk sperm.

The diffusion coefficient D_{motile} was determined as follows. After the sperm injection into the sperm chamber, motile sperm

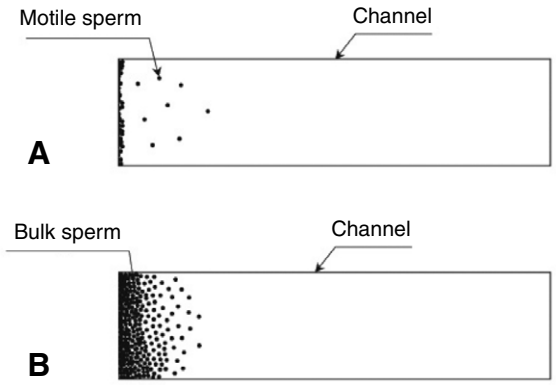

Fig. 2. Schematic of highly motile (A) and bulk (B) sperm in the migration channel. (A) The situation immediately after sperm injection in the sperm chamber. After ~1.5–3 min, the bulk of spermatozoa appear in the migration channel (B). The highly motile sperm shown in A move forward and go out of the focus view by the time bulk sperm appear in the migration channel.

were observed using a 10× eyepiece. The time (t_m) taken by the fastest of the motile sperm to travel the length of view (L) was recorded. The value of D_{motile} was obtained using the first principle of random walk (see section below: *Analysis of sperm diffusivity*).

The diffusion coefficient D was determined as follows. After the time recording of highly motile sperm, the spermatozoa were allowed to diffuse into the channel. The image of the diffused spermatozoa in the migration was captured after ~10–15 min using a digital CCD camera (Orca-ER, Hamamatsu, Hamamatsu City, Japan) at 200× and Simple PCI software (C.IMAGE Systems, Compix Inc. Imaging Systems, Cranberry Township, PA, USA), ensuring that the spermatozoa diffused in the migration channel were motile and the spermatozoa were imaged well before the end of the observed lifetime of sperm in ASW (~30 min) or sperm in resact and jelly coat/ASW samples (~20 min). Appendix C describes the details of the sperm lifetime experiments. The time t at which the image was captured was also recorded. The spermatozoa images were analyzed using ImageJ image processing software [Version 1.34s (Macintosh), National Institutes of Health, Bethesda, MD, USA] to obtain the D value (see sections below: *Image processing* and *Analysis of sperm diffusivity*).

The D_{motile} and D values of the spermatozoa in resact and jelly coat/ASW were also obtained using the above procedures. The prepared microfluidic device was filled with resact solutions and jelly coat solutions, and the sperm samples for these experiments were prepared in the respective solutions (resact or jelly coat/ASW). For each sperm sample (ASW, resact solution and jelly coat solution), the diffusion experiment was carried out three times and three images of the diffusing spermatozoa were obtained as well as three time readings for the D_{motile} estimation. After each set of experiments, the microfluidic device was filled with the sperm sample and its image was captured immediately. For all experiments, care was taken to record the diffusing spermatozoa prior to reaching the observed lifespan in each medium. This was motivated by our reuse of the microfluidic devices, which become irretrievably fouled with sperm death, since dead sperm got bonded to the channel walls and could not be removed.

Image processing

The camera-captured images of diffusing sperm were processed using ImageJ so as to obtain the data that were required to determine the D values. The intensities in the gray scale units (as obtained by ImageJ on a scale of 255 for red, blue and yellow) of the spermatozoa images were used for this purpose. Diffused sperm appeared dark against the light background under the inverted microscope; thus, in the inverted image they would appear bright against the dark background and the value of light intensity would be proportional to sperm concentration. During experimentation, the level of the microscope focus was set to capture as many sperm as possible. These images were then opened using ImageJ, and using the ImageJ functions, 'Find Edges', 'Sharpen', 'Binary' and 'Invert', the spermatozoa were adjusted to appear as bright spots against a perfectly black background. These operations ensured that only sperm contributed to the average value of intensity (I), at a given location in the image. These intensity values were used to determine the D values and the procedure was as follows.

Once the camera-captured image was processed, the scale of the image was set using the known 500 μm width of the migration channel. Then the zone of the migration channel showing diffused sperm was divided into small rectangular sub-zones using the 'rectangle' button available in ImageJ. The width of these rectangular sub-zones ranged from 29.5 to 31.5 μm (a schematic of the placement of those rectangles is shown in Fig. 3). Once a rectangle was created, the average value of light intensity (I) in that rectangle and the location of the center of that rectangle along the length (x) of the channel were recorded. The I and x values were collected for all such rectangular sub-zones. The obtained I values were normalized (I_n) using the light intensity (I_0) of the sperm sample.

The I_0 value for each sperm sample (sperm/ASW, sperm/resact and sperm/jelly coat solutions) was obtained using the corresponding sperm sample image. The sperm sample images were recorded after the respective diffusion experiments. The captured sperm sample image was opened using ImageJ, and subjected to the processes as described above. Then the average light intensity values were measured at three different locations, by drawing three rectangles in the migration channel. The I_0 value for a sperm sample was then obtained by calculating the average value of the three light intensity measurements. The I_n *vs* x data and solution to the diffusion equation were used to obtain the diffusion coefficient values for bulk sperm, as explained in the next section.

Analysis of sperm diffusivity

The D_{motile} value was calculated using published equations (Berg, 1993; Tompkins and Pinnel, 1971):

$$D_{motile} = \frac{L^2}{2t_m}, \quad (1)$$

where L is the observation length, and t_m is time required by the

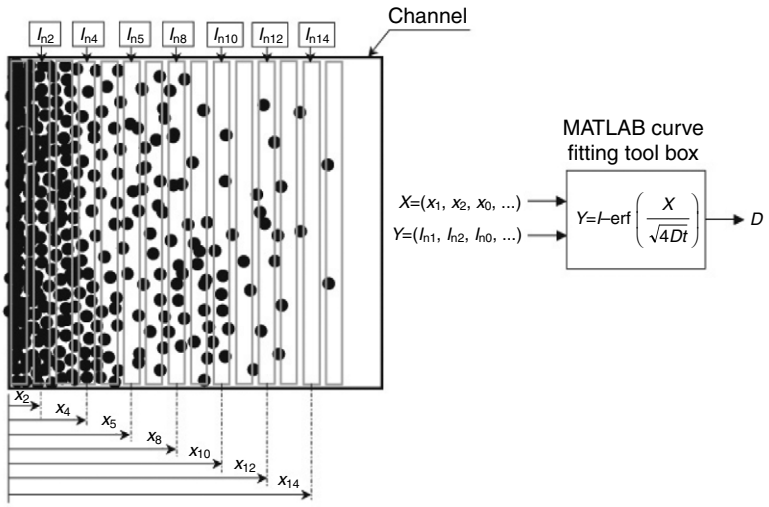

Fig. 3. An illustration of the methodology employed to estimate the diffusion coefficient values of bulk sperm (*D* value). The processed image showing diffused bulk sperm is divided into small rectangular zones (gray rectangles) of 29.5–31.5 μm width. The average light intensity of each rectangular zone (*I* value) and the location of its center along the length of the channel (*x* value) are recorded. The *I* values are normalized (called I_n values and shown in the figure) using the intensity value of the corresponding sample (I_o value). The *x* values as *X* coordinates and I_n values as *Y* coordinates are supplied to the MATLAB curvefitting toolbox. The *D* value is obtained by curve-fitting Eqn 6 to the I_n–*x* data. Not all I_n and *x* values are shown for the sake of clarity. erf, error function.

fastest of the highly motile spermatozoa to traverse the length *L*.

The *D* value was obtained using the solution to the diffusion equation. Because the dimensions of the cross section of the channel were very small compared to its length [0.5 mm (width) and 0.1 mm (height) ⩽7 mm (length), see Fig. 1], sperm diffusion in the channel was treated as one-dimensional. The sperm injection in the sperm chamber was modeled as application of sudden concentration ρ_0 at one end of the channel, with the governing partial differential equation:

$$\frac{\partial\rho(x,t)}{\partial t} = D\,\frac{\partial^2\rho(x,t)}{\partial x^2}\,, \tag{2}$$

where *t* is time, *x* is the coordinate along the length of the channel, and $\rho(x,t)$ is the sperm density value in the channel at time *t* at location *x*.

The boundary condition for this problem was:

$$\rho(x,t) = \rho_0 \text{ for } x=0\,, \tag{3}$$

with the initial condition:

$$\rho(x,t) = 0 \text{ for } x>0 \text{ and } t=0\,. \tag{4}$$

The solution to Eqn 2 can be obtained to be:

$$\frac{\rho(x,t)}{\rho_0} = 1 - \text{erf}\left(\frac{x}{\sqrt{4Dt}}\right), \tag{5}$$

where erf is an error function. As described in the previous section, image processing was carried out to obtain the contribution of sperm concentration in the form of light intensity. Hence Eqn 5 was modified to use the obtained intensity data within this framework as:

$$\frac{\rho(x,t)}{\rho_0} = \frac{I}{I_0} = 1 - \text{erf}\left(\frac{x}{\sqrt{4Dt}}\right). \tag{6}$$

Eqn 6 and MATLAB curvefitting toolbox (MCFT) were used to estimate the *D* values using the data obtained from image processing (Fig. 3). The normalized *I* values, i.e. I_n ($I_n=I/I_0$), the corresponding *x* values and the time at which the image was captured (*t*) were inputs to the MCFT. The (I_n,*x*) data were curve fitted using Eqn 6 to obtain the *D* value.

Stochastic simulations

Our prior mobile trap algorithm (Inamdar et al., 2007), which directly simulates probabilistic collisions between two types of mobile particles, was used for these simulations. Sperm–egg collisions comprise a special case of the type of problems handled by this algorithm, with one stationary type of particle (egg) and another, motile type of particle (a spermatozoon). For efficiency, the relative motions of eggs and sperm in simulations were modeled using a single, fixed egg and multiple, moving, non-overlapping sperm. Sperm moved randomly with positions assessed in time increments calculated to be the minimum required for observation of a collision event, i.e. according to the 'first-passage' technique (Inamdar et al., 2007; Lee et al., 1989; Torquato and Kim, 1989).

The dimensions of the system were as follows. The sea urchin egg was assumed to be spherical, with a core diameter (D_C) of 68 μm (Thomas and Bolton, 1999) and a jelly coat thickness of δ (5 μm for the unhydrated egg condition and 24.5 μm for the hydrated egg condition). The simulated domain was a periodic, $1\times1\times1$ mm^3 cube, selected because the resact gradient extends 1 mm around the egg (Kirkman-Brown et al., 2003). Individual spermatoza were modeled as spheres of 4 μm diameter (Harvey, 1956).

Calculation of time increments in simulations was performed as follows. From the current spermatozoa positions, the minimum distance between the center of a spermatozoon and the center of the egg, d_1, was determined. A sphere of radius *r*, calculated as:

$$r = d_1 - 0.5D_C - \delta\,, \tag{7}$$

was constructed around all spermatozoa. The spermatozoa were then moved to a random point on the surface of their respective sphere, with the time step (d*t*) given by:

$$\text{d}t = \frac{r^2}{6D}\,. \tag{8}$$

These steps were repeated for the simulation time of 1800 s

(30 min), or until all spermatozoa hit the egg. The number of sperm–egg collisions was recorded and each sperm–egg collision was considered a fertilization event. Fig. 4 shows a typical path of a spermatozoon toward the egg.

Two sets of collision simulations were performed, for the various values of D_{motile} and D. The experimental D_{motile} and D values were used for this purpose; these values are also reported with other experimental values in the section *Sperm diffusion coefficients* in Results. The D_{motile} values were 2.11×10^{-8} m^2 s^{-1}, 4.64×10^{-8} m^2 s^{-1} and 5.03×10^{-8} m^2 s^{-1}, which corresponded to the D_{motile} values of sperm in ASW, 250 nmol l^{-1} resact and 250× jelly coat/ASW solutions, respectively. The D values were 3.24×10^{-11} m^2 s^{-1}, 1.25×10^{-10} m^2 s^{-1} and 2.98×10^{-10} m^2 s^{-1}, which corresponded to the D values of sperm in ASW, 250 nmol l^{-1} resact and 500× jelly coat/ASW solutions, respectively.

The numbers of spermatozoa were different in resact and jelly coat solutions, i.e. 10 and 30 for the D_{motile}, and 60 and 120 for the D values, respectively. These values were arrived at as follows. For simulations with highly motile sperm, the number of spermatozoa was counted according to the procedure used for the sperm life experiments. The number of spermatozoa in Fig. 5B was first counted using the portion of the channel ahead of bulk sperm. The same window size was used for the spermatozoa counting in Fig. 6B and Fig. 7B. The ratio of the number of spermatozoa in the chemoattractant sample to the number of spermatozoa in the ASW sample was found to be 3 for the resact sample and 2.87 for the jelly coat sample. Hence 10 and 30 spermatozoa were used for simulations with the D_{motile} values. The base number of 10 was used because approximately 10 spermatozoa were observed during the observations of highly motile sperm. For simulations with bulk sperm, the intensity estimations used for the D calculations were averaged for the sperm images in Fig. 5B, Fig. 6B and Fig. 7B. Then the ratio of number of spermatozoa was calculated using the following equation:

$$\frac{n_{chemo}}{n_{ASW}} = \frac{I_{ASW}t_{ASW}}{I_{chemo}t_{chemo}}, \quad (9)$$

where I_X is the average intensity of the sperm sample in X and t_X is the time at which the image was captured. Using Eqn 9, the ratio of number of spermatozoa for 250 nmol l^{-1} resact sample was 2 and for the 250 dilution jelly coat was 1.8. The value of 2 was used and the numbers 60 and 120 were used to obtain the simulation results quickly. It was found that all highly motile spermatozoa collided with the egg before the simulation time limit of 30 min (1800 s) was reached in all cases studied. Hence the ratio of the time required for all 10/30 spermatozoa to hit the egg and 1800 s was used as a measure of sperm–egg collision frequency (referred as normalized collision time). However, not all of the bulk spermatozoa collided with the egg, and thus, the number of sperm–egg collisions, normalized by the initial number of spermatozoa, was used as the measure of sperm–egg collision frequency (referred as normalized number of collisions). For each case, 30 simulations were carried out.

Statistical analyses of experimental data

Statistical analyses were carried out to test the null hypotheses. Our null hypothesis for the experimental data was that the chemoattractants (jelly coat and resact) did not affect the diffusion coefficient values. For this study, a confidant bound of 95%, or P=0.05, was selected to be significant. One-way analysis of variance (ANOVA) was performed using SPSS (SPSS Inc., Chicago, IL, USA) to compare the diffusion coefficients of sperm in the chemoattractant solutions first. Then the diffusion coefficients of sperm in ASW were compared with the diffusion coefficients of sperm in chemoattractant solutions. Whenever there were more than two groups present for the comparison, the data were also analyzed using the Tukey *post-hoc* test.

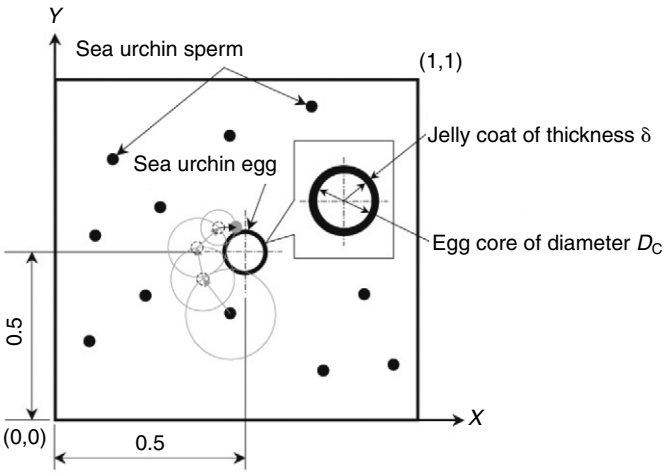

Fig. 4. Schematic of egg–sperm collision simulations. The egg is pinned at the center of the domain, and spermatozoa are distributed randomly at the beginning of the simulation. Then sperm are moved within the domain until they collide (penetrate) the jelly coat.

Results

Sperm diffusion coefficients

We begin by reporting the diffusion coefficients of sperm in ASW. The D_{motile} and D values of sperm diffusing in ASW are shown in Table 2. The average diffusion coefficients of highly motile and bulk sperm in ASW are 2.11×10^{-8} m^2 s^{-1} and 3.24×10^{-11} m^2 s^{-1}, respectively. Fig. 5A–C shows the position of the diffused sperm in ASW and the sperm concentration profile. Bulk sperm are visible at the left end of the channel. Highly motile sperm are not visible in these images because they had traversed the observable length by the time this image was captured.

The diffusion coefficient values of sperm in the jelly coat solutions follow. The D_{motile} and D values of sperm diffusing in various jelly coat solutions are shown in Table 3. The average D_{motile} values of sperm samples in 750×, 500× and 250× diluted jelly coat solutions are 4.73×10^{-8} m^2 s^{-1}, 3.53×10^{-8} m^2 s^{-1} and 5.03×10^{-8} m^2 s^{-1}, respectively. The average D values for sperm samples in 750×, 500× and 250× diluted jelly coat solutions are 1.84×10^{-10} m^2 s^{-1}, 2.98×10^{-10} m^2 s^{-1} and 2.05×10^{-10} m^2 s^{-1}, respectively. Fig. 6A–C shows the position of sperm diffusing in 10:250 dilution jelly coat/ASW solution and the sperm concentration profile. This figure shows that the bulk sperm have diffused to

Table 2. *D_{motile} and D values obtained by conducting the diffusion experiments with the sperm–ASW samples*

Sample no. (description)	Experiment	Highly motile sperm			Bulk sperm	
		t_m (s)	L (μm)	D_{motile} (m^2 s^{-1})	t (s)	D (m^2 s^{-1})
031-31-03 (dry sperm/ASW)	1	89	2017.2	2.29×10^{-8}	897	5.79×10^{-11}
	2	98	2205.47	2.48×10^{-8}	905	4.53×10^{-11}
	3	111	2153.34	2.09×10^{-8}	–	–
	4	133	2205.47	1.82×10^{-8}	–	–
031-31-04 (dry sperm/ASW)	1	110	2205.47	2.21×10^{-8}	907	1.10×10^{-11}
	2	115	2017.2	1.76×10^{-8}	960	2.35×10^{-11}
	3	–	–	–	982	2.25×10^{-11}

–, value was not determined.

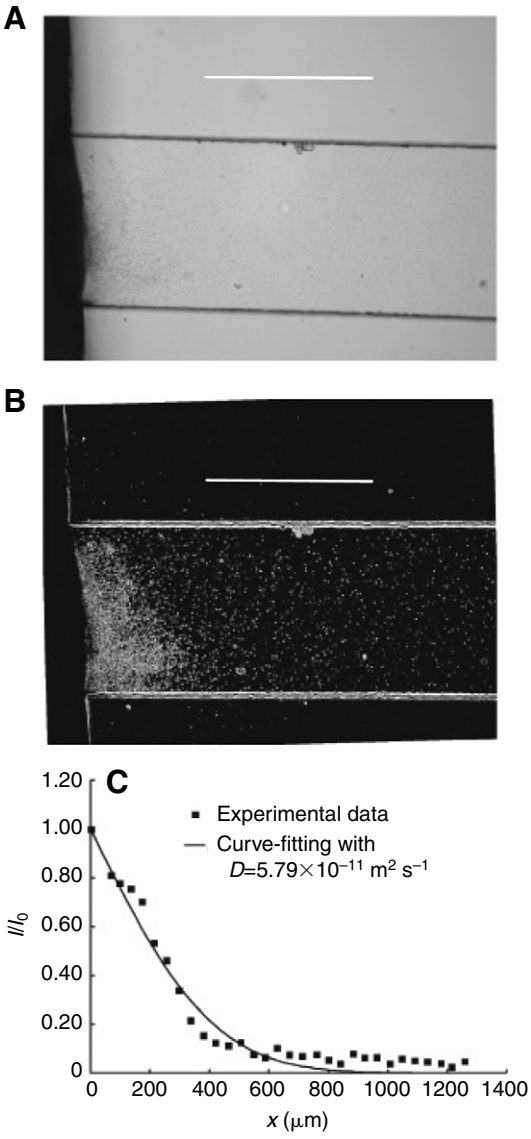

Fig. 5. The captured image (A) and processed image (B) of sperm diffusing in ASW. The sperm sample was prepared by mixing 10 μl dry sperm in 200 μl ASW. (C) The sperm concentration profile along the length of the channel and the *D* value estimation by curve-fitting Eqn 6. Scale bars, 500 μm.

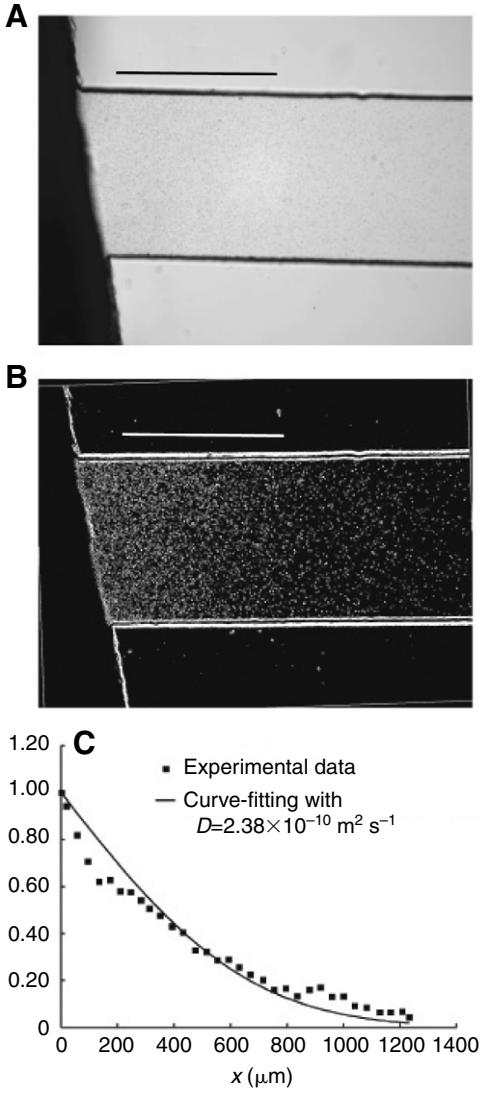

Fig. 6. The captured (A) and processed (B) image of sperm diffusing in 10:250 dilution jelly coat solution. The sperm sample was prepared by mixing 10 μl dry sperm with 200 μl 10:250 dilution jelly coat solution. (C) The sperm concentration profile along the length of the channel and *D* value estimation by curve-fitting Eqn 6. Scale bars, 500 μm.

Table 3. *D_{motile} and D values obtained by conducting the diffusion experiments with the sperm-jelly coat/ASW samples*

Sample no. (description)	Experiment	Highly motile sperm			Bulk sperm	
		t_m (s)	L (μm)	D_{motile} ($m^2 s^{-1}$)	t (s)	D ($m^2 s^{-1}$)
031-37-02 (dry sperm/10:750 jelly coat)	1	40	2205.47	6.08×10^{-8}	563	2.07×10^{-10}
	2	60	2205.47	4.05×10^{-8}	567	1.84×10^{-10}
	3	60	2205.47	4.05×10^{-8}	667	1.60×10^{-10}
031-34-03 (dry sperm/10:500 jelly coat)	1	62	2205.47	3.92×10^{-8}	–	–
	2	71	2205.47	3.42×10^{-8}	485	3.28×10^{-10}
	3	75	2205.47	3.24×10^{-8}	694	2.68×10^{-10}
031-40-02 (dry sperm/10:250 jelly coat)	1	46	2205.47	5.29×10^{-8}	–	–
	2	51	2205.47	4.77×10^{-8}	570	2.38×10^{-10}
	3	–	–	–	698	1.72×10^{-10}

–, value was not determined.

a greater extent and sperm in the migration channel are more homogeneous compared to sperm in the resact solutions and ASW.

Finally, we report the diffusion coefficient values of sperm in the resact solutions. The D_{motile} and D values of sperm diffusing in 25 nmol l^{-1} and 250 nmol l^{-1} resact are shown in Table 4. The average diffusion coefficient of 25 nmol l^{-1} resact–sperm samples is 4.56×10^{-11} $m^2 s^{-1}$ and the average diffusion coefficient of highly motile sperm is 2.08×10^{-8} $m^2 s^{-1}$. The average diffusion coefficient of 250 nmol l^{-1} resact–sperm samples is 1.25×10^{-10} $m^2 s^{-1}$, while that of highly motile sperm is 4.64×10^{-8} $m^2 s^{-1}$. Fig. 7A–C shows the position of sperm diffusing in 250 nmol l^{-1} resact solution and the sperm concentration profile. Bulk sperm are less dense compared to those in ASW samples though there are isolated clusters of sperm present in the channel. Fig. 8A–C shows the position of sperm diffusing in 25 nmol l^{-1} resact solution and the sperm concentration profile. In this case too, bulk sperm are not as dense as those in the sperm–ASW experiments.

The behavior of highly motile and bulk sperm can be summarized as follows. The diffusion coefficient of highly motile sperm in ASW is three orders of magnitude greater than that of bulk sperm. When exposed to resact, the lower concentration of resact solution (25 nmol l^{-1}) apparently affected only the motility of bulk sperm while the higher concentration (250 nmol l^{-1}) appeared to increase the diffusion coefficients of highly motile and bulk sperm. When sperm were exposed to the solutions of jelly coat/ASW, sperm did segregate into highly motile and bulk groups but bulk sperm were not as dense as sperm in ASW (i.e. were cluster free). Significantly, the overall motility of sperm was increased in the presence of the jelly coat solutions, by an order of magnitude over the diffusion coefficient values in ASW (i.e. 2.29×10^{-10} $m^2 s^{-1}$, the average value of all diffusion coefficients of the jelly coat-treated sperm, *versus* 3.24×10^{-11} $m^2 s^{-1}$, the diffusion coefficient of sperm in ASW).

Statistical analysis of the experimental data

Table 5A shows the P values corresponding to the diffusion coefficients of sperm treated with all three jelly coat/ASW solutions. Table 5B shows the P values corresponding to the diffusion coefficients of sperm in ASW and the jelly coat/ASW solutions. Table 6A shows the P values corresponding to the diffusion coefficients of sperm in 25 nmol l^{-1} and 250 nmol l^{-1} resact concentrations. Table 6B shows the P values corresponding to the diffusion coefficients of sperm in ASW and resact concentrations. The diffusion coefficient values presented in Table 2, Table 3 and Table 4 were used for ANOVA but only average values are shown in Table 5 and Table 6 for the sake of clarity.

Table 4. *D_{motile} and D values obtained by conducting the diffusion experiments with the sperm-resact samples*

Sample no. (description)	Experiment	Highly motile sperm			Bulk sperm	
		t_m (s)	L (μm)	D_{motile} ($m^2 s^{-1}$)	t (s)	D ($m^2 s^{-1}$)
031-34-04 (dry sperm/25 nmol l^{-1} resact)	1	80	2017.2	2.54×10^{-8}	666	6.63×10^{-11}
	2	93	2017.2	2.19×10^{-8}	–	–
	3	110	2017.2	1.85×10^{-8}	816	4.82×10^{-11}
	4	116	2017.2	1.75×10^{-8}	960	2.22×10^{-11}
031-37-03 (dry sperm/250 nmol l^{-1} resact)	1	59	2017.2	3.45×10^{-8}	599	0.70×10^{-10}
031-42-01 (dry sperm/250 nmol l^{-1} resact)	1	41	2017.2	5.93×10^{-8}	471	1.85×10^{-10}
	2	51	2017.2	4.77×10^{-8}	701	1.19×10^{-10}
	3	55	2017.2	4.42×10^{-8}	–	–

–, value was not determined.

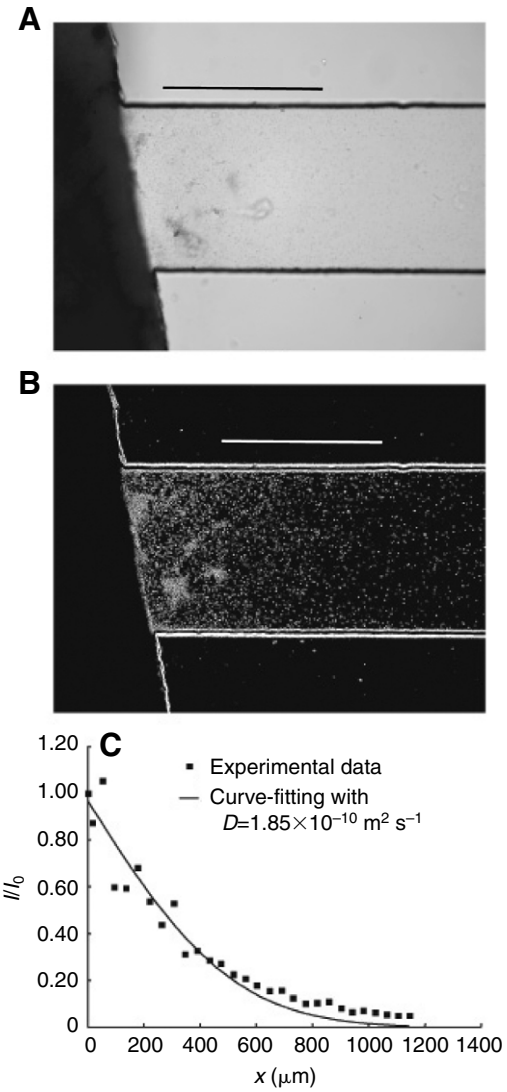

Fig. 7. The captured image (A) and processed image (B) of sperm diffusing in 250 nmol l^{-1} resact solution. The sperm sample was prepared by mixing 10 μl dry sperm with 200 μl 250 nmol l^{-1} resact solution. (C) The sperm concentration profile along the length of the channel and the D value estimation by curve-fitting Eqn 6. Scale bars, 500 μm.

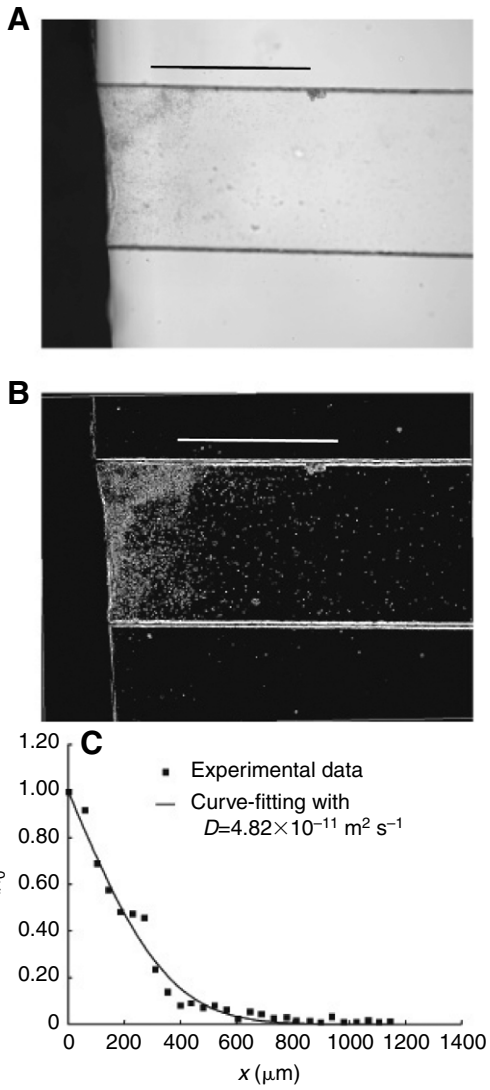

Fig. 8. The captured image (A) and processed image (B) of sperm diffusing in 25 nmol l^{-1} resact solution. The sperm sample was prepared by mixing 10 μl dry sperm with 200 μl 25 nmol l^{-1} resact solution. (C) The sperm concentration profile along the length of the channel and the D value estimation by curve-fitting Eqn 6. Scale bars, 500 μm.

Stochastic simulations

The data obtained from the simulations are presented in Fig. 9. Fig. 9A shows the simulation data obtained using highly motile sperm. In this figure the normalized collision times are plotted as a function the normalized diffusion coefficients (or normalized diffusivity) of highly motile sperm. The normalized diffusivity values are obtained using the following equation:

$$D_{\mathrm{n}} = \frac{\sqrt{D_{\mathrm{motile}} t_{\mathrm{sim}}}}{\phi_{\mathrm{egg}}}, \qquad (10)$$

where t_{sim} is the stipulated simulation time (1800 s) and ϕ_{egg} is the egg diameter. The values of the normalized collision times plotted on y-axis are average values. Fig. 9B shows the simulation data obtained using bulk sperm. Here the normalized number of collisions is plotted as a function of the normalized diffusivities of bulk sperm. The normalized diffusivity values are obtained using Eqn 10 with the D values replacing the D_{motile} values. The other two parameters in Eqn 10 remain the same. The values of the normalized number of collisions plotted on y-axis are the average values. In both the figures, the points on the graph are connected to illustrate the trend only.

Discussion

Comparison of this work with the earlier work

This work represents the treatment of sperm motility and fertilization in *Arbacia punctulata*, through parallel comparative analytical (continuum) and stochastic simulation studies. Though sperm motility has been examined previously in *Arbacia punctulata* (Ward et al., 1985; Kaupp et al., 2003),

Table 5. *P values corresponding to the diffusion coefficients of (A) sperm–jelly coat/ASW samples and (B) sperm–ASW and sperm–jelly coat/ASW samples*

(A) Variable (mean values)	10:250 jelly coat/ASW	10:500 jelly coat/ASW	10:750 jelly coat/ASW	*P* value
D_{motile} ($m^2 s^{-1}$)	5.03×10^{-8}	3.53×10^{-8}	4.73×10^{-8}	0.16
D ($m^2 s^{-1}$)	2.05×10^{-10}	2.98×10^{-10}	1.84×10^{-10}	0.06

(B) Variable (mean values)	ASW	Jelly coat/ASW	*P* value
D_{motile} ($m^2 s^{-1}$)	2.11×10^{-8}	4.43×10^{-8}	0.0002
D ($m^2 s^{-1}$)	3.24×10^{-11}	2.29×10^{-10}	$<10^{-3}$

effective diffusion coefficients have not been reported. And, though continuum solutions have been applied to 2D sperm motion (Riedel et al., 2005) of *Strongylocentrotus sroebachiensis* and *S. purpuratus* and the diffusion coefficient of the sperm vortex has been measured as 6.2 $\mu m^2 s^{-1}$, they have not been applied to this species, nor examined through stochastic approaches. Finally, stochastic simulations (Inamdar et al., 2007) have been implemented for problems ranging from the intracellular transport to the generalized chemical reactions data but none have been reported for this application using the experimental values. Existing sperm–egg collision modeling techniques are based on chemical kinetics (Vogel et al., 1982; Farley, 2002), but still they do not use the diffusion coefficient of the spermatozoa.

Importance of sperm type to characterize diffusion coefficients

The present study focused on the effects of three main factors on diffusion of sperm: sperm type and the effects of two types of chemoattractants (jelly coat and purified resact). The first of these factors was serendipitous, from initial studies of sperm in ASW, i.e. that sperm segregate into bulk and highly motile sperm groups. Throughout the remainder of the study, then, we separately studied effects of the chemoattractants on these groups, in terms of altered diffusion coefficients. Our results showed that the bulk and the highly motile groups in fact behaved significantly differently and the diffusion coefficients of highly motile sperm were always 2–3 orders of magnitude higher than those of bulk sperm. Also, highly motile sperm are first to reach eggs, and thus are given greater importance.

Effect of chemoattractants on sperm diffusion coefficients

The second factor studied was the effect of the jelly coat/ASW solutions on the diffusion coefficient values. The diffusion coefficient values of the jelly coat/ASW treated sperm were higher than the diffusion coefficient values of sperm in ASW alone. In the case of highly motile sperm, this increase was ~2 times and in the case of bulk sperm, the increase was by an order of magnitude (Table 5B). However, there was no significant effect of the concentration of the jelly coat/ASW on the diffusion coefficient values of sperm (Table 5A). These observations suggest that even when diluted 750×, the jelly coat saturated the spermatozoa [a spermatozoon saturates when 50–100 resact molecules bind it (Kaupp et al., 2003)]. Also it has been observed that the spermatozoa did not show sensitivity to resact when the spermatozoa were treated with 1 $\mu mol\ l^{-1}$ resact (Ward et al., 1985). Hence, the insensitivity of the spermatozoa to three dilutions of the jelly coat/ASW solutions shows that the amount of resact present in these dilutions is probably of the order of $\mu mol\ l^{-1}$. There is also a possibility of presence of other peptides in the jelly coat that assist sperm in uptake of resact. The ability of the spermatozoa to diffuse uniformly (Fig. 6) compared to the resact-only treated spermatozoa (Fig. 7 and Fig. 8) appears to support this idea. Because of the possibility of this dual role of the jelly coat, this increase in the diffusion coefficient values is an important factor.

The third factor studied was the effect of the resact solutions on the diffusion coefficient values of sperm. The diffusion experiments showed that the 25 $nmol\ l^{-1}$ resact slightly affected bulk sperm but 250 $nmol\ l^{-1}$ resact affected bulk as well as highly motile sperm (Table 6B). The range of resact concentrations (25 $nmol\ l^{-1}$–250 $nmol\ l^{-1}$) used in this study gives an idea about the threshold value of resact concentration that affects highly motile as well as bulk sperm. Ward et al. had observed that the spermatozoa responded differently when the resact concentration value exceeded 3.3 $nmol\ l^{-1}$ (Ward et al.,

Table 6. *P values corresponding to the diffusion coefficients of (A) sperm–resact samples and (B) sperm–ASW and sperm–resact samples*

(A) Variable (mean values)	25 $nmol\ l^{-1}$ resact	250 $nmol\ l^{-1}$ resact	*P* value
D_{motile} ($m^2 s^{-1}$)	2.08×10^{-8}	4.64×10^{-8}	0.0033
D ($m^2 s^{-1}$)	4.56×10^{-11}	1.25×10^{-10}	0.09

(B) Variable (mean values)	ASW	25 $nmol\ l^{-1}$ resact	250 $nmol\ l^{-1}$ resact	*P* value
D_{motile} ($m^2 s^{-1}$)	2.11×10^{-8a}	2.08×10^{-8a}	4.64×10^{-8}	6.81×10^{-5}
D ($m^2 s^{-1}$)	3.24×10^{-11b}	4.56×10^{-11b}	1.25×10^{-10}	0.05

The same superscript letters indicate no significant difference between the marked groups.

1985) but the authors studied the local behavior of the spermatozoa. The threshold resact value required for the spermatozoa to exhibit a different behavior on the aggregate scale appears to be between 25 nmol l^{-1} – 250 nmol l^{-1}. Also the diffusion coefficients (D_{motile} and D) of 250 nmol l^{-1} resact-treated highly motile sperm are close to those of the jelly coat/ASW-treated sperm (Table 5 and Table 6). This observation, when viewed in conjunction with the observed insensitivity of the spermatozoa to the jelly coat dilutions, suggests that 250 nmol l^{-1} resact contains enough resact molecules to almost saturate the number of spermatozoa present in 10 μl solution, and induce the maximum possible chemokinetic effect.

Effect of two types of sperm targeting the egg on sperm–egg collision frequency

Because of the experimental observations that sperm segregating into two types, namely highly motile and bulk, the simulations were carried out in two separate sets, with D_{motile} values characterizing highly motile sperm and D values characterizing bulk sperm. The simulation results also showed differences in behavior. Because of their higher diffusion coefficients, motile sperm that collided with the egg well before the sperm lifetime of 30 min was reached (the maximum average collision time was less than 20% of the simulation time). But, not all bulk sperm collided with the egg; the maximum number of bulk sperm collided with the egg was 61, corresponding to the jelly coat/ASW bulk sperm and the big egg. Hence two different measures were used to characterize the collision frequency, namely (1) for highly motile sperm, the fraction of 30 min required for all spermatozoa to collide with the egg and (2) for bulk sperm, the number of sperm–egg collisions before the sperm lifetime of 30 min was reached. This number was normalized by the initial number of spermatozoa.

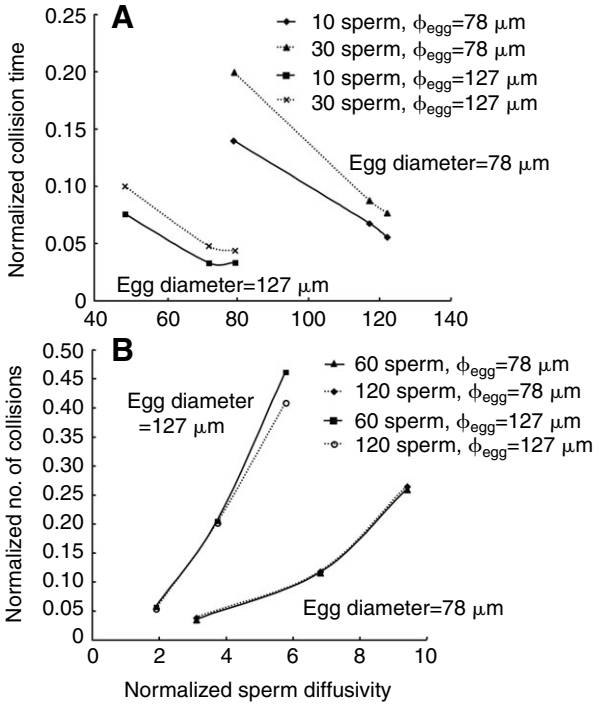

Fig. 9. Presentation of the sperm–egg collision data using dimensionless variables. (A) The highly motile sperm–egg collision data. The normalized sperm diffusion coefficient values are obtained using $\sqrt{D_{motile}t_{sim}/\phi_{egg}}$, where t_{sim} is the simulation time (1800 s) and ϕ_{egg} is the egg diameter. The normalized collision times are the ratio of time required for 10/30 highly motile sperm to collide the egg, to the simulation time. The values along *y*-axis are the average collision time values. (B) The bulk sperm–egg collision data. The normalized sperm diffusion coefficient values are obtained using $\sqrt{Dt_{sim}/\phi_{egg}}$, where t_{sim} is the simulation time (1800 s) and ϕ_{egg} is the egg diameter. The normalized number of collision values are obtained by dividing the number of bulk sperm hitting the egg in 1800 s by the initial number of sperm. The values along *y*-axis are average values of number of collisions. Lines joining data points show trends only.

Effect of number of spermatozoa on sperm–egg collision frequency

Experimentation with the chemoattractant-treated spermatozoa showed that the number of spermatozoa that appeared in the migration channel were different when compared with diffusion of the sperm samples in ASW. The two different numbers of spermatozoa (10 and 30 for highly motile sperm; 60 and 120 for bulk sperm) represent the extent of resact and jelly coat/ASW solutions affecting the spermatozoa. Fig. 9A shows that, for a given egg diameter and the number of spermatozoa, the normalized collision time decreases with the increase in sperm diffusivity. Also the data corresponding to 10 and 30 spermatozoa follow similar trends. As expected, the data for 30 spermatozoa lie above the data for 10 spermatozoa. As the diffusion coefficient of sperm increases, the two sets of data come close to each other, in each group.

Fig. 9B, on the other hand, reveals a very interesting phenomenon. For a given egg diameter, the normalized number of sperm–egg collisions *vs* the normalized sperm diffusivity data, for both the number of spermatozoa, run close to each other. Noting that only one sperm–egg collision is required for successful fertilization of an egg, and increase in the diffusion coefficient values of sperm was considerable in the presence of resact and jelly coat, the number of spermatozoa is not a significant factor for highly motile or for bulk sperm.

The effect of increase in diffusion coefficient on sperm–egg collision frequency

The diffusion coefficient was the third factor considered for simulations, because experiments showed that the chemoattractants (jelly coat and resact) increased the diffusion

Table 7. *The normalized (dimensionless) collision times of highly motile sperm, shown for different values of egg diameter, number of spermatozoa and normalized sperm diffusivity*

	Number of spermatozoa=10			Number of spermatozoa=30		
ND (D_{motile})	6.16 (2.11×10^{-8})	9.14 (4.64×10^{-8})	9.52 (5.03×10^{-8})	6.16 (2.11×10^{-8})	9.14 (4.64×10^{-8})	9.52 (5.03×10^{-8})
ϕ_{egg}=78 μm	**29.6**	**30.6**	**28.9**	**35.3**	**34.7**	**33.9**
ϕ_{egg}=127 μm	**13.4**	**13.1**	**13.7**	**15.3**	**15.8**	**15.7**

N_t (shown in **bold**), normalized collision time; ND, normalized sperm diffusivity; ϕ_{egg}, egg diameter (78 μm = unhydrated egg; 127 μm = egg with hydrated jelly coat).

The dimensionless collision time, N_t, is constant for a given value of egg diameter and number of spermatozoa, and hence cannot be used to reveal the effect of increase in the diffusion coefficient values in presence of the chemoattractants. N_t and ND values were calculated using

$$N_t = \frac{\sqrt{D_{motile} \times t_{collision}}}{\phi_{egg}} \quad \text{and} \quad ND = \frac{\sqrt{D_{motile} \times t_{sim}}}{L},$$

where D_{motile} ($m^2\,s^{-1}$) is the diffusion coefficient of highly motile sperm, L is the length of simulation domain (1 mm), t_{sim} is the simulation time (30 min), $t_{collision}$ is the average time required for all 10/30 sperm to collide the egg and ϕ_{egg} is the egg diameter.

coefficient values of highly motile as well as bulk sperm. Three values of diffusion coefficient were used to represent sperm in ASW, 250 nmol l^{-1} resact and in jelly coat/ASW solutions. The effect of increase in sperm diffusivity on sperm–egg collisions can be clearly seen in Fig. 9. For highly motile sperm (Fig. 9A) the effect of increase in sperm diffusivity is significant for the smaller egg. But for bulk sperm (Fig. 9B), the effect of increase in sperm diffusivity is significant for the larger egg. The significance in both the cases is evident for a given egg size (small or large). These simulation results suggest that highly motile and bulk sperm, coupled with the effect of chemoattractants, are parallel mechanisms contributing to successful fertilization regardless of whether the egg is coated with a jelly layer or not.

The effect of increase in egg diameter on sperm–egg collision frequency

Finally the egg diameter was the fourth factor considered for simulations. This factor was used to test the target enlargement hypothesis. The two different values the egg diameter used for simulations were that of unhydrated egg (78 μm) and that of hydrated jelly coat (127 μm). The effect of increase in the egg diameter is clearly revealed in Fig. 9. For highly motile as well as bulk sperm, enlargement of the egg amplifies the effect of increase in sperm diffusivity, in the presence of chemoattractants on sperm–egg collision frequency. Collectively, these observations suggest that the factors considered for simulations (except the number of spermatozoa) work in concert toward successful fertilization of an egg.

These observations, when viewed along with the mechanical protection role of the jelly coat, give some interesting insights. When the jelly coat is intact on eggs, resact molecules will diffuse in the surrounding water affecting the motile sperm. If the egg experiences mechanical loading sufficient to rupture the jelly coat, then the jelly coat will dissolve in the surrounding water and will affect bulk sperm also, giving the exposed egg a greater chance to be fertilized because its cytoskeleton will still be intact. From the stochastic collision simulations, we can see that when the jelly coat is intact, it contributes to enhanced collision frequency by making sperm motile and increasing the egg diameter. But the effect of increasing diffusion coefficient values alone has an equally marked effect on collision frequency with the small egg (being fast is equivalent to being large), and hence the jelly coat also serves a mechanism in increasing the spermatozoa motility as its likely (main) role.

In the present simulation methodology, one value of the diffusion coefficient was assigned to all spermatozoa, assuming that all spermatozoa were affected by resact and jelly coat. Since the simulation domain was $1\times1\times1$ mm^3, this assumption was reasonable because the resact gradient extends 1 mm around the egg (Kirkman-Brown et al., 2003). With a possibility of domains exceeding 1 mm, this assumption needs to be revisited, considering that the resact is a small peptide and may diffuse very fast before the jelly coat completely dissolves. A quantitative study dealing with this situation has not yet been reported, but the present microfluidic channel can be used to test the hypothesis of there being a single, repeatable value for all spermatozoa, by placing eggs in the chemochamber and reducing the length of the migration channel.

Conclusions and future work

Changes in the diffusion coefficients of highly motile and bulk sperm when the spermatozoa are treated with resact and jelly coat/ASW solutions confirm their chemokinetic properties. But the lack of significant differences between the diffusion coefficients of individual jelly coat/ASW treated sperm implies that the jelly coat saturates the spermatozoa. Also, the cluster-like diffusion of the resact-treated spermatozoa (Fig. 7 and Fig. 8, the spermatozoa near the left edge of the channel), may be a selective mechanism for these faster sperm. The 250 nmol l^{-1} resact-treated spermatozoa (Fig. 10A) clearly exhibit this aggregation.

Simulation results showed that for a given number and type of spermatozoa, the increases in diffusion coefficient and egg diameter values increased the collision frequency. Due to low numbers and high diffusion coefficients, all of the highly motile sperm collided with the egg but only a few of the bulk sperm collided with the egg. We can conclude that type of sperm, egg diameter and diffusion coefficient are significant factors in egg

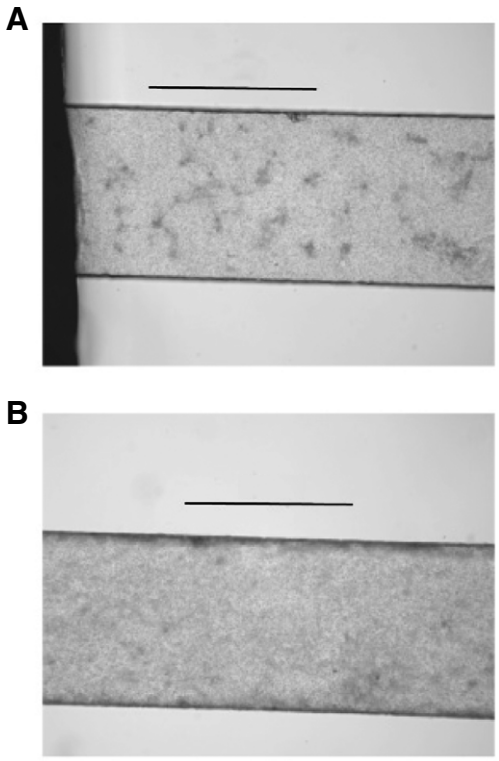

Fig. 10. Images of sperm treated with 250 nmol l^{-1} resact (A) and 10:250 dilution jelly coat (B). The resact sample shows clusters of sperm, which are absent in jelly coat sample. These images were taken immediately after filling the microfluidic device with respective samples. Scale bars, 500 μm.

fertilization. Increasing the motility of sperm appears to be the prominent role of the jelly coat.

The physical conditions of the sea urchins from which gametes were obtained and their diet may affect the spermatozoa behavior. Also there may be other peptides that might be aiding the jelly coat-treated spermatozoa to diffuse homogeneously that are not known. At present we are in the process of using this diffusive device to differentiate between chemokinetic or chemoattractive effects, and have also further planned the diffusion experiments using concentrated jelly coats to determine the maximum limit of the sperm diffusivity.

Finally, the difference between the effective diffusion coefficients of highly motile and bulk sperm motivated us to propose the presence of two types of sperm. A biochemical assay that detects the cellular activities (such as Ca^{2+} or cGMP activities) of these sperm, obtained using the present microfluidic device, could be developed to understand the differences between these types of sperm. Though beyond the scope of the present work, a careful study would entail consideration of phenotype and genotype, and a thorough investigation of analogs of such observations in other species. While we have not done so as yet, we find that the very high levels of significance observed in differences between these two groups may have important implications for reproductive endocrinology, and merit a targeted study.

Appendix A

Preparation of media for the microfluidic experiments

Artificial seawater (ASW) was prepared by dissolving synthetic sea salt (Aquarium Systems, Mentor, OH, USA) in distilled water to 33–34 p.p.t. salinity. Jelly coat solutions were prepared by dissolving the jelly coats around dry eggs in ASW as follows. 500 μl ASW were added to the vial containing dry eggs and the mixture was then shaken gently for 5 min. The status of the jelly coats around eggs was checked using Sumi ink, which does not penetrate the jelly coat, and thus can be used to locate intact jelly coats (light) around eggs (dark). After most of the eggs jelly coats had dissolved, the solution was held at 4°C for 24 h, whereupon the number of eggs present in 0.5 μl of the egg–water solution was counted. An average of 75.5 eggs per 0.5 μl was counted for 4 drops containing 78, 73, 75 and 76 eggs, respectively. The egg–water solution was then centrifuged (Centrifuge 5415D, Eppendorf, Westbury, NY, USA) three times, at 1000, 2000 and 2000 r.p.m. for 2 min, respectively, whereupon the separated jelly coat solution was stored in a separate vial at 4°C and reserved as the 'parent' jelly coat solution. Three jelly coat dilutions were prepared from the parent jelly coat solution including 10:250, 10:500 and 10:750 dilutions prepared by mixing 10 μl of the parent jelly coat solution with 240, 490 and 740 μl of ASW, respectively.

Resact solutions of various concentrations were prepared as follows. The solid resact (500 μg as received; Phoenix Pharmaceuticals Inc., Balmont, CA, USA) was first dissolved to 500 μl of final volume for the storage concentration of 1 μg μl^{-1} (8.035×10^{-4} mol l^{-1}). This was done by first adding 200 μl of ASW to the solid resact vial and the final volume of the solute was measured. This intermediate resact solution was diluted to its final volume of 500 μl. The storage solution was later diluted further, to give 250 nmol l^{-1} and 25 nmol l^{-1} resact solutions.

Eight sperm samples for the diffusion experiments were prepared in various concentrations of ASW, jelly coat and resact. One comprised a mixture of 10 μl dry sperm with 200 μl ASW; one comprised a mixture of 10 μl dry sperm with 100 μl ASW; two comprised mixtures of 10 μl of dry sperm with 200 μl of 250 nmol l^{-1} resact; and one comprised 10 μl of dry sperm mixed with 200 μl of 25 nmol l^{-1} resact. The final three samples comprised mixtures of 10 μl of dry sperm with 200 μl of each jelly coat/ASW samples.

Appendix B

Microfluidic apparatus: design and fabrication

The microfluidic apparatus used to determine the diffusion coefficients was modified from the versions developed as the

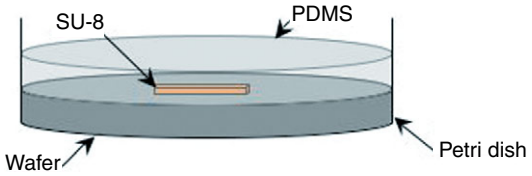

Fig. B1. The schematic of PDMS poured on the silanized wafer with channel features.

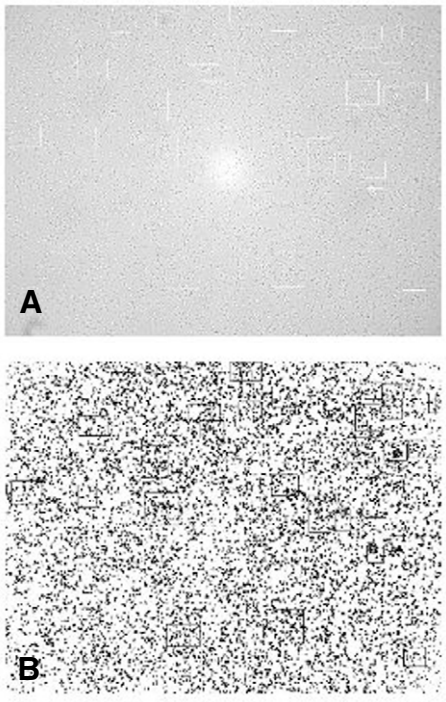

Fig. C1. A typical image of from the sperm life experiments showing immobile sperm among mobile ones. (A) The image captured using the CCD camera and SimplePCI. (B) The image processed by ImageJ. The sperm dilution for this image was 40× and hence the sperm clusters are visible in both the images.

human sperm sorters (Cho et al., 2003; Suh et al., 2003). An SU-8 (negative, near UV, epoxy) photoresist master mold with a rectangular channel was constructed on a silicon wafer *via* photolithography. The patterned wafer was silanized using (Tridecafluoro-1,1,2,2-tetrahydrooctyl)-1-Trichlorosilane (C8H4Cl3F3Si, TFS, United Chemical Technologies Inc., Bristol, PA, USA) using chemical vapor deposition in an evacuated desiccator for 15 min. After silanization, poly(dimethysiloxane) (PDMS; Sylgard 184, Dow Corning, Midland, MI, USA) was first mixed in the 1:10 ratio by weight, debubbled, and then poured on the wafer and cured at 60°C for 1 h. After curing, the resulting PDMS slab with the channel features was detached from the wafer, whereupon two reservoirs were cut, one at each end of the channel, using a crafting knife (X-acto®) (Fig. 1). This PDMS slab with the channel and reservoirs was bonded to another PDMS piece using oxygen plasma treatment. The bonding surfaces of both the pieces were oxidized for 30 s using 40 mA current and 66.65 kPa pressure, under oxygen plasma (SPI Supplies, West Chester, PA, USA), followed by hermetic sealing. The sealed device was then incubated at 60°C in an oven for 1.5 h to ensure complete, permanent bonding. The schematic of the procedure is shown in Fig. B1.

Appendix C

Experimental determination of sperm lifetime

Two different sperm dilutions were prepared in the ASW for these experiments. Dry sperm, obtained as above, were diluted 40 times by mixing 2.5 μl of dry sperm with 100 μl of the ASW. This dilution yielded less motile and dense sperm. The second dilution was obtained by mixing 2.5 μl of dry sperm with 1000 μl of the ASW (400× dilution). This dilution yielded isolated highly motile sperm. All diluted samples were prepared immediately before microscopy and dry sperm were stored in a 4°C refrigerator between the experiments.

The microscopy procedure was as follows. Sperm samples were observed under an inverted microscope (TS 100, Nikon, Melville, NY, USA) using an assembly of BIOCOAT poly-D-lysine 2-well Cultureslide (Becton Dickinson and Company, Franklin Lakes, NJ, USA) and a glass slide. First, the plastic walls of the culture slide were removed. The glass culture slide was then rinsed thoroughly and dried and the poly-D-lysine coating was removed. The blue bonding material around the glass slide provided a height of approximately 50 μm through which sperm could move. Before each sperm life experiment, a

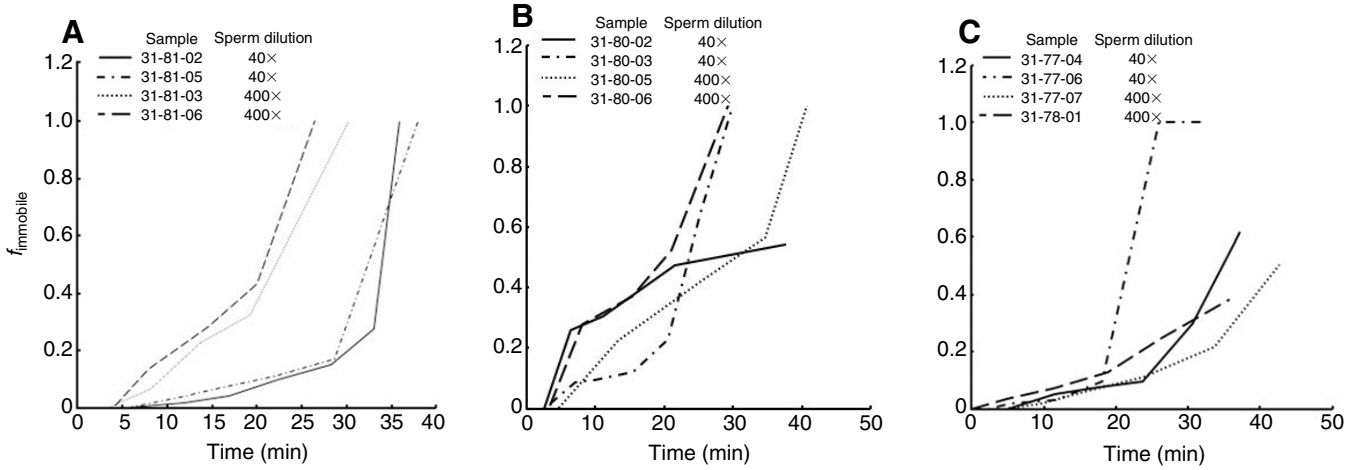

Fig. C2. The fraction of immobile sperm shown as a function of time. (A–C) These three graphs were obtained for sperm from three sea urchins (shown separately in A, B and C). The fraction of immobile sperm is shown for both the sperm dilutions, 40× and 400×. The data for all sperm samples studied for the sperm life experiments are shown in these figures.

freshly diluted sperm sample was prepared and the time of dilution recorded. A 2.5 μl sample of the diluted sperm was placed onto the BIOCOAT 2-well Cultureslide and covered with a microscope slide. The covering prevented crystallization of sperm samples. The sperm sample was then placed under an inverted microscope (TS 100, Nikon) and the sample was imaged using a CCD camera (Hamamatsu Orca-ER) and SimplePCI software (Compix Inc. Imaging Systems). During imaging, the microscope was focused so as make the entire sperm sample visible. The sperm sample was observed until sperm were immobile. Images were captured every ~5–10 min, using SimplePCI. Before capturing each image, immobile sperm were annotated using rectangles or ellipses drawing buttons available in SimplePCI. Some experiments were terminated after 40 min, so as to analyze the dry sperm sample immediately. Two sets of images were collected for each sperm dilution. After the experiment the device was taken off the microscope, cleaned and rinsed for the next experiment. The fraction of mobile sperm as a function of time was obtained using the collected images as described below.

Image processing was performed using ImageJ image processing software [Version 1.34s (Macintosh), National Institutes of Health]. Images captured using SimplePCI were saved in the JPEG 8-bit Gray format and subsequently processed using ImageJ. Sperm and annotated boundaries in the image were extracted using the '*Find Edges*' function. Then the image was inverted using the '*Threshold*' function. This operation converted sperm into dark spots on white background. The total pixel count of an image was calculated using the '*Analyze Particles*' function (N_1). This value included contribution from mobile sperm, immobile sperm and the annotated boundaries. The pixel count of the immobile sperm located inside the annotated rectangles was determined by using the free hand selection tool and '*Analyze Particles*' function (N_2). The pixel count of the annotated boundaries and the interior sperm was also determined (N_3) using the same procedure. And finally, using the freehand selection tool, ~10 sperm were selected and their pixel values were averaged to determine the number of pixels/sperm. For each image, using the number of pixels/sperm value, the N_1, N_2 and N_3 values were converted into the number of sperm values and the fraction immobile sperm was calculated using:

$$f_{\text{immobile}} = N_2 / (N_1+N_2-N_3) . \quad \text{(C1)}$$

For each sample, f_{immobile} as a function of time was plotted to study the time-dependent behavior of the fraction of sperm immobile. Fig. C1A shows a SimplePCI image with the annotated rectangles; sperm inside the rectangles are immobile. Fig. C1B shows the processed image. Sperm can be seen as black spots on a white background. Fig. C2 shows the fraction of immobile sperm as a function of time for three sea urchins. Each figure corresponds to the experiments on sperm of one animal. Low and high dilution sperm samples exhibited separate trends with sperm in 400× dilution samples reaching complete immobility in 25–27 min while sperm in 40× dilution samples reaching complete immobility in 35–37 min (Fig. C2A). High and low dilution sperm samples did not show separate trends and sperm became immobile in 30–40 min (Fig. C2B). Fig. C2C also shows similar results except for one 40× dilution sperm sample. Sperm in the other three samples did not become completely immobile. These experiments were stopped after 40 min. Based on the findings of these experiments, the diffusion experiments were run for 10–15 min to ensure that more than 80% of the spermatozoa would be mobile.

Support for this work provided by ONR/DARPA Synthetic Multifunctional Materials Program, Dr Leo Christodoulou and Dr Steve Fishman, Program Monitors (Sastry), and HIMB contribution no. 1281 (Thomas), is gratefully acknowledged. Computations were performed on a Sun Fire Cluster V480, a gift of Sun Microsystems, Incorporated (Lastoskie, Sastry). The authors also gratefully acknowledge this equipment support.

References

Adler, J. (1969). Chemoreceptors in bacteria. *Science* **166**, 1588-1597.

Adler, J. (1973). Method for measuring chemotaxis and use of method to determine optimum conditions for chemotaxis by *Escherichia coli*. *J. Gen. Microbiol.* **74**, 77-91.

Berg, H. C. (1993). *Random Walks in Biology*. Princeton, NJ: Princeton University Press.

Brown, S., Poole, P. S., Jeziorska, W. and Armitage, J. P. (1993). Chemokinesis in *Rhodobacter sphaeroides* is the result of a long term increase in the rate of flagellar rotation. *Biochim. Biophys. Acta* **1141**, 309-312.

Chalub, F., Markowich, P. A., Perthame, B. and Schmeiser, C. (2004). Kinetic models for chemotaxis and their drift-diffusion limits. *Monatsh. Math.* **142**, 123-141.

Chen, K. C., Ford, R. M. and Cummings, P. T. (1999). Spatial effect of tumbling frequencies for motile bacteria on cell balance equations. *Chem. Eng. Sci.* **54**, 593-617.

Chen, K. C., Ford, R. M. and Cummings, P. T. (2003). Cell balance equation for chemotactic bacteria with a biphasic tumbling frequency. *J. Math. Biol.* **47**, 518-546.

Cho, B. S., Schuster, T. G., Zhu, X. Y., Chang, D., Smith, G. D. and Takayama, S. (2003). Passively driven integrated microfluidic system for separation of motile sperm. *Anal. Chem.* **75**, 1671-1675.

Cook, S. P., Brokaw, C. J., Muller, C. H. and Babcock, D. F. (1994). Sperm chemotaxis: egg peptides control cytosolic calcium to regulate flagellar responses. *Dev. Biol.* **165**, 10-19.

D'Orsogna, M. R., Suchard, M. A. and Chou, T. (2003). Interplay of chemotaxis and chemokinesis mechanisms in bacterial dynamics. *Phys. Rev. E* **68**, 021925-1-10.

Farley, G. S. (2002). Helical nature of sperm swimming affects the fit of fertilization-kinetics models to empirical data. *Biol. Bull.* **203**, 51-57.

Farley, G. S. and Levitan, D. R. (2001). The role of jelly coats in sperm–egg encounters, fertilization success, and selection on egg size in broadcast spawners. *Am. Nat.* **157**, 626-636.

Ford, R. M. and Lauffenburger, D. A. (1991). Analysis of chemotactic bacterial distributions in population migration assays using a mathematical model applicable to steep or shallow attractant gradients. *Bull. Math. Biol.* **53**, 721-749.

Ford, R. M., Phillips, B. R., Quinn, J. A. and Lauffenburger, D. A. (1991). Stopped-flow chamber and image-analysis system for quantitative characterization of bacterial population migration – motility and chemotaxis of *Escherichia coli* K12 to fucose. *Microb. Ecol.* **22**, 127-138.

Harvey, E. N. B. (1956). The *American Arbacia and Other Sea Urchins*. Princeton, NJ: Princeton University Press.

Hill, N. A. and Häder, D. P. (1997). A biased random walk model for the trajectories of swimming micro-organisms. *J. Theor. Biol.* **186**, 503-526.

Hillen, T. (1996). A Turing model with correlated random walk. *J. Math. Biol.* **35**, 49-72.

Hultin, E. (1956). Mechanism of fertilization by rate determinations. *Exp. Cell Res.* **10**, 286-293.

Inamdar, M. V., Lastoskie, C. M., Fierke, C. A. and Sastry, A. M. (2007). Mobile trap algorithm for zinc detection using protein sensors. *J. Chem. Phys.* (in press).

Kaupp, U. B., Solzin, J., Hildebrand, E., Brown, J. E., Helbig, A., Hagen, V., Beyermann, M., Pampaloni, F. and Weyand, I. (2003). The signal flow and motor response controling chemotaxis of sea urchin sperm. *Nat. Cell Biol.* **5**, 109-117.

Kirkman-Brown, J. C., Sutton, K. A. and Florman, H. M. (2003). How to attract a sperm. *Nat. Cell Biol.* **5**, 93-96.

Lauffenburger, D., Ads, R. and Keller, K. H. (1981). Effects of random motility on growth of bacterial populations. *Microb. Ecol.* **7**, 207-227.

Lee, S. B., Kim, I. C., Miller, C. A. and Torquato, S. (1989). Random-walk simulation of diffusion-controlled processes among static traps. *Phys. Rev. B* **39**, 11833-11839.

Lewus, P. and Ford, R. M. (2001). Quantification of random motility and chemotaxis bacterial transport coefficients using individual-cell and population-scale assays. *Biotechnol. Bioeng.* **75**, 292-304.

MacNab, R. M. (1996). Flagella and motility. In *Escherichia Coli and Salmonella Typhimurium: Cellular and Molecular Biology* (ed. F. C. Neidhardt), Chapter 10. Washington, DC: ASM Press.

Parkinson, J. S. (1993). Signal transduction schemes of bacteria. *Cell* **73**, 857-871.

Podolsky, R. D. (2001). Evolution of egg target size: an analysis of selection on correlated characters. *Evolution* **55**, 2470-2478.

Podolsky, R. D. (2002). Fertilization ecology of egg coats: physical versus chemical contributions to fertilization success of free-spawned eggs. *J. Exp. Biol.* **205**, 1657-1668.

Podolsky, R. D. (2004). Life-history consequences of investment in free-spawned eggs and their accessory coats. *Am. Nat.* **163**, 735-753.

Ralt, D., Manor, M., Cohen-Dayag, A., Tur-Kaspa, I., Ben-Shlomo, I., Makler, A., Yuli, I., Dor, J., Blumberg, S., Mashiach, S. et al. (1994). Chemotaxis and chemokinesis of human spermatozoa to follicular factors. *Biol. Reprod.* **50**, 774-785.

Richards, G. R., Millard, R. M., Leveridge, M., Kerby, J. and Simpson, P. B. (2004). Quantitative assays of chemotaxis and chemokinesis for human neural cells. *Assay Drug Dev. Technol.* **2**, 465-472.

Riedel, I. H., Kruse, K. and Howard, J. (2005). A self-organized vortex array of hydrodynamically entrained sperm cells. *Science* **309**, 300-303.

Rivero, M. A., Tranquillo, R. T., Buettner, H. M. and Lauffenburger, D. A. (1989). Transport models for chemotactic cell populations based on individual cell behavior. *Chem. Eng. Sci.* **44**, 2881-2897.

Rothschild and Swann, M. M. (1951). The fertilization reaction in the sea-urchin – the probability of a successful sperm–egg collision. *J. Exp. Biol.* **28**, 403-416.

Roush, C. J., Lastoskie, C. M. and Worden, R. M. (2006). Denitrification and chemotaxis of *Pseudomonas stutzeri* KC in porous media. *J. Environ. Sci. Health A Tox. Hazard Subst. Environ. Eng.* **41**, 967-983.

Schmidt, S., Widman, M. T. and Worden, R. M. (1997). A laser-diffraction capillary assay to measure random motility in bacteria. *Biotechnol. Tech.* **11**, 423-426.

Schnitzer, M. J. (1993). Theory of continuum random-walks and application to chemotaxis. *Phys. Rev. E* **48**, 2553-2568.

Schuel, H. (1984). The prevention of polyspermic fertilization in sea-urchins. *Biol. Bull.* **167**, 271-309.

Shimomura, H. and Garbers, D. L. (1986). Differential effects of Resact analogs on sperm respiration rates and cyclic-nucleotide concentrations. *Biochemistry* **25**, 3405-3410.

Shimomura, H., Suzuki, N. and Garbers, D. L. (1986). Derivatives of Speract are associated with the eggs of *Lytechinus pictus* sea urchins. *Peptides* **7**, 491-495.

Stock, J. B. and Surette, M. G. (1996). Chemotaxis. In *Escherichia Coli and Salmonella Typhimurium: Cellular and Molecular Biology* (ed. F. C. Neidhardt), Chapter 73. Washington, DC: ASM Press.

Suh, R. S., Phadke, N., Ohl, D. A., Takayama, S. and Smith, G. D. (2003). Rethinking gamete/embryo isolation and culture with microfluidics. *Human Reproduction Update* **9**, 451-461.

Suzuki, N. and Garbers, D. L. (1984). Stimulation of sperm respiration rates by Speract and Resact at alkaline extracellular pH. *Biol. Reprod.* **30**, 1167-1174.

Suzuki, N., Shimomura, H., Radany, E. W., Ramarao, C. S., Ward, G. E., Bentley, J. K. and Garbers, D. L. (1984). A peptide associated with eggs causes a mobility shift in a major plasma-membrane protein of spermatozoa. *J. Biol. Chem.* **259**, 4874-4879.

Thomas, F. I. M. and Bolton, T. F. (1999). Shear stress experienced by echinoderm eggs in the oviduct during spawning: potential role in the evolution of egg properties. *J. Exp. Biol.* **202**, 3111-3119.

Thomas, F. I. M., Edwards, K. A., Bolton, T. F., Sewell, M. A. and Zande, J. M. (1999). Mechanical resistance to shear stress: the role of echinoderm egg extracellular layers. *Biol. Bull.* **197**, 7-10.

Thomas, F. I. M., Bolton, T. F. and Sastry, A. M. (2001). Mechanical forces imposed on echinoid eggs during spawning: mitigation of forces by fibrous networks within egg extracellular layers. *J. Exp. Biol.* **204**, 815-821.

Tompkins, H. G. and Pinnel, M. R. (1971). Relative rates of nickel diffusion and copper diffusion through gold. *J. Appl. Phys.* **48**, 3144-3146.

Torquato, S. and Kim, I. C. (1989). Efficient simulation technique to compute effective properties of heterogeneous media. *Appl. Phys. Lett.* **55**, 1847-1849.

Vacquier, V. D. (1998). Evolution of gamete recognition proteins. *Science* **281**, 1995-1998.

Vogel, H., Czihak, G., Chang, P. and Wolf, W. (1982). Fertilization kinetics of sea-urchin eggs. *Math. Biosci.* **58**, 189-216.

Ward, G. E., Brokaw, C. J., Garbers, D. L. and Vacquier, V. D. (1985). Chemotaxis of *Arbacia punctulata* spermatozoa to Resact, a peptide from the egg jelly layer. *J. Cell Biol.* **101**, 2324-2329.

Widman, M. T., Emerson, D., Chiu, C. C. and Worden, R. M. (1997). Modeling microbial chemotaxis in a diffusion gradient chamber. *Biotechnol. Bioeng.* **55**, 191-205.

Wilkinson, P. C. (1990). How do leucocytes perceive chemical gradients? *FEMS Microbiol. Immunol.* **64**, 303-312.